

From Optimal Planning to Visual Servoing With Limited FOV

Paolo Salaris*, Lucia Pallottino*, Seth Hutchinson†, Antonio Bicchi*‡

Abstract—This paper presents an optimal feedback control scheme to drive a vehicle equipped with a limited Field-Of-View (FOV) camera towards a desired position following the shortest path and keeping a given landmark in sight. Based on the shortest path synthesis available from previous works, feedback control laws are defined for any point on the motion plane exploiting geometric properties of the synthesis itself. Moreover, by using a slightly generalized stability analysis setting, which is that of stability on a manifold, a proof of stability is given. Reported simulations demonstrate the effectiveness of the proposed technique.

I. INTRODUCTION

Visual servoing techniques use visual information directly, by the computation of an image error signal, or indirectly, by the evaluation of the state of the vehicle (see [1] and [2]). These two approaches, often referred to as Image-Based and Position-Based visual servoing ([3]), can be regarded as the end-points of a range of different possibilities. However, few practical problems still affect visual servoing approaches and depend on the particular available robotic set-up. For example, in case of limited Field-Of-View (FOV) cameras, the problem is of maintaining in sight the features necessary for the visual servoing during the robot manoeuvres. In [4] and in [5] authors present a visual control approach consisting in a switching control scheme based on the epipolar geometry. Anyway, whereas [4] does not consider the problem of keeping the features in the FOV, in [5] it is assumed that difference in depth from the initial position to the goal is greater than the side distance from the initial position to the goal, avoiding the need of high rotations. On the other hand, in [6] authors propose a visual control where the advantages of position-based visual servoing and image-based visual servoing are merged, and a hybrid error vector is defined. In this case the camera FOV constraints are alleviated because the algorithm works well with few feature points. In the context of mobile robotics, the FOV problem has been successfully solved for a unicycle-like vehicle in [7], [8], [9] but, the resultant path is inefficient and not optimal.

In this paper we consider the problem of visual servo control for a unicycle-like vehicle equipped with a monocular fixed vision system. The system, subject to nonholonomic constraints imposed by the vehicle kinematics and to FOV

constraints imposed by camera, must reach a desired position on the motion plane following the optimal (shortest) path. In order to localize itself and to compute a visual servo control, the robot must keep at least three features in view. Indeed given three or more features both in the current image and in the desired one, by using the estimation technique proposed in [6], state variables of the vehicle are available up to a scale factor. A first step toward the solution of this problem has been done in [10] and [11] considering a single feature to be kept in sight. In these papers, a shortest path synthesis (locally and globally valid, respectively) has been provided, i.e., a partition of the motion plane into regions completely describing the shortest path type from any starting point in that region to the goal point. An optimal synthesis in case of three or more features in view is still under study.

Towards the practical application of the results of these works, a crucial step is to translate the optimal trajectories (which are evaluated from any initial condition as plans to be executed in open-loop) into feedback control laws, i.e., to write laws which determine the control inputs (the vehicle velocities) as a function of the current state of the system only. Only when such a feedback control law is derived, it will be possible to make the system reach the desired posture with robustness against disturbances and uncertainties, i.e., it will be possible to show *stability* of the system at the desired configuration.

A first result in this direction has been reported in [12]. Based on the locally optimal synthesis in [10], rewritten in terms of the parameters of the homography matrix, the authors of [12] provide a visual control law based on an iterative steering scheme, which is a generalized form of feedback control (cf. e.g., [13]). The authors discuss the stability of the method. However, as we will discuss later on in this paper (see the example in remark 1 in section III), the application of any feedback control scheme congruent with the optimal synthesis in [10] and [11] is not — strictly speaking — stabilizing the final posture in the sense of Lyapunov.

In [14], an algorithm to translate the optimal (shortest) paths synthesis to the image plane, thus enabling a purely image-based optimal control scheme has been proposed. In that paper, the optimal trajectory is analytically computed from the initial position of the robot to the desired one directly on the image plane. Then, a purely image-based standard feedback trajectory controller tracking the optimal path is given minimizing the feature error between the actual trajectory and the reference one. However, the planned path on the image plane was affected by noise and hence, a replanning during the path was necessary whenever an

*The research leading to these results has received funding from the European Union Seventh Framework Programme [FP7/2007-2013] under grant agreement n257462 HYCON2 Network of excellence”.

* Interdept. Research Center “Enrico Piaggio”, University of Pisa, Italy. p.salaris, l.pallottino, bicchi@centropiaggio.unipi.it,

† Dept. of Electrical and Computer Engineering, Beckman Institute for Advanced Science and Technology, University of Illinois, USA seth@uiuc.edu, ‡Department of Advanced Robotics, Istituto Italiano di Tecnologia, via Morego, 30, 16163 Genova, Italy

updating of the actual position of the robot was available. In this paper, based on the geometric properties of the optimal synthesis in [11], optimal feedback control laws, which are able to align the vehicle to the shortest path from the current configuration, are defined for any point on the motion plane. These laws are provided in explicit form as simple algebraic functions of the current state only, which can be easily computed to give in real time the velocity input to be used - thus requiring no replanning procedure, and being intrinsically more robust. Also, the method does not require the use of homography, thus being computationally cheaper and not causing ambiguities. Stability properties for the proposed control scheme are proven in a properly generalized analysis setting, which is that of stability on a manifold [15], and by using a generalization of LaSalle's invariance principle for discontinuous righthand system [16]. Finally, based on a visual control scheme where a combination of position-based visual servoing and image-based visual servoing are merged, simulation results are reported to show the effectiveness of the proposed technique.

II. PROBLEM DEFINITION

Let us consider a vehicle moving on a plane where a right-handed reference frame $\langle W \rangle$ is defined with origin in O_W and axes X_W, Z_W . The configuration of the vehicle is described by $\xi(t) = (x(t), z(t), \theta(t))$, where $(x(t), z(t))$ is the position in $\langle W \rangle$ of a reference point in the vehicle, and $\theta(t)$ is the vehicle heading with respect to the X_W axis (see figure 1). We assume that the dynamics of the vehicle are negligible, and that the forward and angular velocities, $v(t)$ and $\omega(t)$ respectively, are the control inputs to the kinematic model of the vehicle.

Choosing polar coordinates for the vehicle $\eta = [\rho \ \psi \ \beta]^T$ (see figure 1) the kinematic model of the unicycle-like robot is

$$\begin{bmatrix} \dot{\rho} \\ \dot{\psi} \\ \dot{\beta} \end{bmatrix} = \begin{bmatrix} -\cos \beta & 0 \\ \frac{\sin \beta}{\rho} & 0 \\ \frac{\sin \beta}{\rho} & -1 \end{bmatrix} \begin{bmatrix} v \\ \omega \end{bmatrix}. \quad (1)$$

We consider vehicles with bounded velocities that can turn on the spot. In other words, we assume

$$(v, \omega) \in U, \quad (2)$$

with U a compact and convex subset of \mathbb{R}^2 , containing the origin in its interior. The vehicle is equipped with a rigidly fixed pinhole camera with a reference frame $\langle C \rangle = \{O_c, X_c, Y_c, Z_c\}$ such that the optical center O_c corresponds to the robot's center $[x(t), z(t)]^T$ and the optical axis Z_c is aligned with the robot's forward direction.

Because we will frequently be interested only in the projection of η onto the robot's workspace, i.e., in the polar coordinates of the origin of the robot's frame $\langle C \rangle$, we introduce the notation $Q = (\rho, \psi)$ as a shorthand notation.

Let us assume that the feature to be kept within the on-board camera FOV is placed on the axis through the origin O_W and perpendicular to the plane of motion. Moreover, we

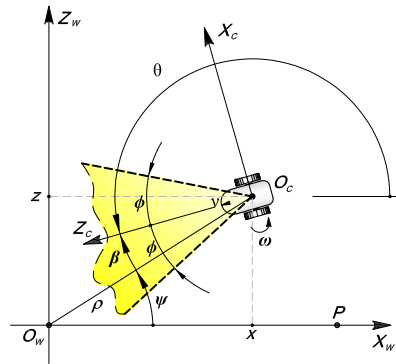


Fig. 1: Mobile robot and systems coordinates. The robot's task is to reach P while keeping O_W within a limited FOV (shaded in figure).

consider a symmetric planar FOV with characteristic angle $\delta = 2\phi$, that generates the constraints

$$\beta + \phi \geq 0, \quad \beta - \phi \leq 0. \quad (3)$$

Notice that, in this context, we do not take under consideration vertical FOV limits. Therefore, the height of the feature on the motion plane, which corresponds to its Y_c coordinate in the camera frame $\langle C \rangle$, is irrelevant to this problem. Hence, it is necessary to know only the projection of the feature on the motion plane, i.e., O_W .

Without loss of generality, we assume desired position P of the robot to lay on the X_W axis, with coordinates $(\rho, \psi) = (\rho_P, 0)$ and with $\beta \in \mathcal{W} = [-\phi, \phi]$, where $\phi \in]0, \pi/2[$.

Let us consider the following optimal control problem: for any point $Q \in \mathbb{R}^2$ in the robot space to P , to minimize the length of the path covered by the center of the vehicle by keeping the feature anytime in sight, i.e., minimizing the cost functional

$$L = \int_0^\tau |v| dt, \quad (4)$$

under the *feasibility constraints* (1), (2), (3). Here, τ is the time needed to reach P that is $\rho(\tau) = \rho_P, \psi(\tau) = 0$.

Previous papers on this subject have studied this problem ([11], [10], [17]). They provide a complete optimal synthesis, i.e., a language of optimal control words, and a global partition of the motion plane induced by shortest paths, such that a word in the optimal language is univocally associated to a region and completely describes the shortest path from any starting point in that region to the goal point. For reader convenience, next section is dedicated to briefly summarize the work presented in [11].

A. Shortest Path Synthesis

In this section, we report main results of [11] referring to this paper for further details.

As a first result, based on the theory of optimal control with state and control constraints [18], extremal maneuvers of the optimal problem (i.e. maneuvers that satisfy necessary conditions for optimality) are rotation on the spot (corresponding to $v = 0$ and denoted by $*$), straight

line (corresponding to $\omega = 0$ and denoted by S), and two logarithmic spirals with characteristic angle ϕ , clockwise and counterclockwise rotating around the feature (i.e., O_W) and denoted by T^L and T^R , respectively. Moreover, as extremal arcs can be executed by the vehicle in either forward or backward direction, we use superscripts $+$ and $-$ to make this explicit (e.g., S^- stands for a straight line executed backward w.r.t. the heading angle). In conclusion, extremal paths consist of sequences, or *words*, comprised of symbols in the alphabet $\{*, S^+, S^-, T^{R+}, T^{R-}, T^{L+}, T^{L-}\}$. Rotations on the spot ($*$) have zero length, but may be used to properly connect other maneuvers. A concatenation of type TS (ST) refers to a smooth transition.

Symmetries and invariants of the problem have been exploited to determine optimal paths from any point of the motion plane to the goal, providing a complete partition of the motion plane in regions as shown in figure 2 and described in Table I. Despite that every optimal path may begin and end with a turn on the spot, in Table I, we omit explicit mention of initial and final rotation in place to simplify notation.

Let us also introduce here a further result of [11] which will turn out to be a useful tool in the following sections. For any point Q , let us consider region C_Q delimited by two circle arcs C_Q^R and C_Q^L between Q and O_W such that $\forall V \in C_Q^R (C_Q^L)$, angle $\widehat{QVO_W} = \pi - \phi$ in the half-plane on the right (left) of $\overline{QO_W}$. We will refer to $C_Q^R (C_Q^L)$ as the right (left) ϕ -arc in Q . Moreover, let $r_Q^R (r_Q^L)$ denote the half-line from Q forming an angle $\psi_Q + \phi$ ($\psi_Q - \phi$) with the X_W axis. Also, let Γ_Q denote the cone delimited by r_Q^R and r_Q^L . We will refer to $r_Q^R (r_Q^L)$ as the right (left) ϕ -radius in Q . By elementary geometric arguments, all points of C_Q and Γ_Q are reachable by a straight line without violating the FOV constraints. Moreover, we have the following result whose proof can be found in [11]:

Proposition 1: If an optimal path from Q includes a segment of the type S^+ (S^-), with extremes in A and B (B and A), then either $B = P \in C_A$ ($A = P \in C_B$) or $B \in C_A^R \cup C_A^L$ ($A \in r_B^R \cup r_B^L$).

Before starting toward desired position P , vehicle needs to localize itself in the motion plane, that is to deduce the region it belongs to, in order to select the optimal path. For any point $Q = (\rho, \psi)$, i.e., the current robot position, Table I describes the criteria to deduce the region Q belongs to, based on ratio ρ/ρ_P and angle ψ .

The computation of these parameters requires at least two corresponding features in the current image and in the desired one in addition to the one that must be maintained inside FOV during all maneuvers that vehicle performs from Q to P , along shortest path. Indeed, in [19] authors show that, by taking the planar motion constraint of the mobile robot into account, robot position can be directly computed using three feature points in a non singular configuration, up to a common scale factor arbitrarily chosen within the set of state variable (for example, the height of one feature w.r.t. $\langle C \rangle$ frame).

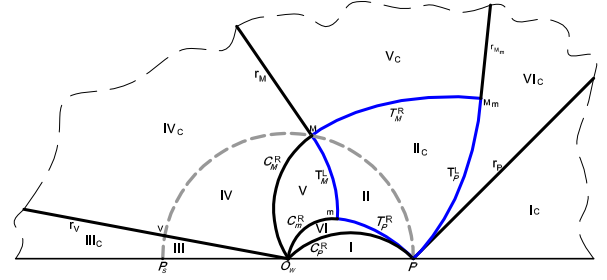


Fig. 2: Partition of the upper half plane with $\phi = \pi/4$.

| Region | Optimal Path Type | Inclusion Conditions |
|-----------------|---------------------------|---|
| I | S^- | $\rho \leq \rho_P \frac{\sin(\phi - \psi)}{\sin \phi}$, and $\psi \leq \phi$ |
| Ic | S^+ | $\rho > \rho_P \frac{\sin \phi}{\sin(\phi - \psi)}$, and $\psi \leq \phi$ |
| II \cup IIc | $T^{L+} * T^{R-}$ | $\rho_P e^{(\psi - \psi_M)t} \leq \rho \leq \rho_P e^{-(\psi - \psi_M)t}$, $\rho_P e^{-\psi t} < \rho < \rho_P e^{\psi t}$, $\psi \leq \psi_M$ |
| II' | T^{R-} | $\rho = \rho_P e^{-\psi t}$, with $\psi \leq \frac{\psi_M}{2}$ |
| IIc' | T^{L+} | $\rho = \rho_P e^{\psi t}$, with $\psi \leq \frac{\psi_M}{2}$ |
| III \cup IIIc | $S^+ * S^-$ | $2\phi + \psi_M \leq \psi \leq \pi$ |
| IV \cup IVc | $S^+ T^{L+} * T^{R-} S^-$ | $\rho_P \frac{\sin \psi}{\sin \phi} \leq \rho \leq \rho_P \frac{\sin \phi}{\sin \psi}$, $\psi_M \leq \psi \leq 2\phi + \psi_M$ |
| V | $T^{L+} * T^{R-} S^-$ | $\rho \leq \rho_P \frac{\sin \psi}{\sin \phi}$, $\rho_P e^{-(\psi_Q - \psi_M)t} \leq \rho \leq \rho_P e^{-(\psi - \psi_M)t}$, $\frac{\psi_M}{2} \leq \psi \leq \psi_M + \phi$ |
| Vc | $S^+ T^{L+} * T^{R-}$ | $\rho_P \frac{\sin \phi}{\sin \psi} \leq \rho \leq \rho_P \frac{1}{\sin \phi \sin \psi}$, $\rho \geq \rho_P e^{-(\psi - \psi_M)t}$, $\frac{\psi_M}{2} \leq \psi \leq \psi_M + \phi$ |
| VI | $T^{R-} S^-$ | $\rho_P \frac{\sin(\phi - \psi)}{\sin \phi} \leq \rho \leq \rho_P \sin \phi \sin \psi$, $\rho \leq \rho_P e^{-\psi t}$, and $\psi \leq \phi + \frac{\psi_M}{2}$ |
| VIc | $S^+ T^{L+}$ | $\rho_P \frac{1}{\sin \phi \sin(\phi - \psi)} \leq \rho \leq \rho_P \frac{\sin \phi}{\sin \psi}$, $\rho \geq \rho_P e^{\psi t}$, and $\psi \leq \phi + \frac{\psi_M}{2}$ |

TABLE I: Optimal synthesis in the upper half-plane and Region inclusion conditions for initial position Q . Where $\tilde{\psi} = \phi - \psi + \psi_M$ and $\hat{\psi} = \phi - \psi + \frac{\psi_M}{2}$.

III. OPTIMAL FEEDBACK CONTROL LAWS

In this section, we define feedback control laws $u(\eta) = [v(\eta), \omega(\eta)]^T$ for any initial configuration $\eta = [\rho, \psi, \beta]^T$ of the vehicle. In this regard, it should be noticed that the shortest path synthesis in Table I is completely defined in terms of variables ρ/ρ_P and ψ only, but it is independent from β . Indeed, the synthesis is obtained minimizing cost functional 4 which does not weigh β . For this reason, the cost functional does not constrain β to be decreasing, as shown in the following remark.

Remark 1: Consider a vehicle position Q , on the boundary C_P^R between Region I and Region VI (see figure 2), arbitrarily close to the desired position P w.r.t. states ρ , ψ , and β . In other words, let $\eta = (\rho_P - \varepsilon_1, \varepsilon_2, \varepsilon_3)$ where ε_1 , ε_2 and ε_3 are arbitrarily small (see figure 3). In order to perform an

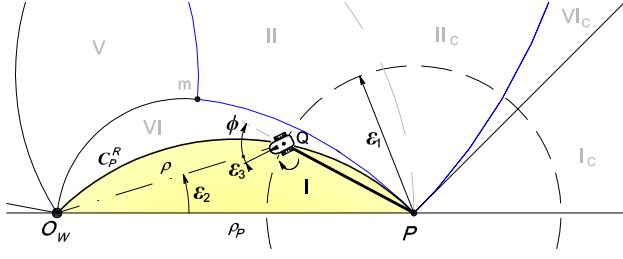


Fig. 3: An example to show that point P is not stable for the optimality controlled system, in the sense of Lyapunov.

optimal path, the vehicle must turn on the spot in Q , and β goes as far as ϕ before converging to zero. This happens for any robot configuration on C_p^R . Thus, strictly speaking, point P is not stable in the sense of Lyapunov for the system controlled with the optimal synthesis in [11] and [10] (the two synthesis coincide here).

Despite the previous remark, the proposed optimal feedback control scheme clearly exhibits convergence and boundedness of trajectories, which can be formalized and proved in a slightly generalized stability analysis setting, which is that of stability on a manifold ([15]). In this regard, let a function $V : \mathbb{R}^3 \rightarrow \mathbb{R}$ be defined as

$$V(\eta) = \frac{1}{2} \left(\frac{\rho}{\rho_P} - 1 \right)^2 + \frac{\psi^2}{2} + \frac{1}{2} D^2(\beta, \mathcal{W}), \quad (5)$$

where $D(\beta, \mathcal{W})$ is defined as

$$D(\beta, \mathcal{W}) = \begin{cases} -\beta - \phi & \text{if } \beta < -\phi, \\ 0 & \text{if } \beta \in \mathcal{W} = [-\phi, \phi], \\ \phi - \beta & \text{if } \beta > \phi. \end{cases} \quad (6)$$

Notice that, (5) is a continuously differentiable function such that $V(\eta) = 0$ on manifold $M = \{\eta \in \mathbb{R}^3 \mid \rho = \rho_P, \psi = 0, \beta \in \mathcal{W}\}$, whereas set

$$\Omega_\ell = \{\eta \in \mathbb{R}^3 : V(\eta) \leq \ell\}$$

is bounded for every $\ell > 0$. In the following, we consider a value ℓ such that set $\{\beta \mid -\pi/2 < \beta < \pi/2\}$ is included inside Ω_ℓ . The time derivative of (5) along the trajectories of the system is given by

$$\dot{V}(\eta) = \frac{1}{\rho_P} \left[- \left(\frac{\rho}{\rho_P} - 1 \right) \cos \beta + (\psi - D(\beta, \mathcal{W})) \frac{\rho_P \sin \beta}{\rho} \right] v + D(\beta, \mathcal{W}) \omega, \quad (7)$$

where v and ω are robot's control inputs. As the vehicle has to be always aligned with the optimal path, ω is determined by geometrical conditions deduced by the synthesis itself. On the other hand, as the vehicle has to reach point P along the shortest path without any time constraint, v can be chosen in order to make \dot{V} at least negative semidefinite, e.g.,

$$v = \bar{v} = -K_v \left[- \left(\frac{\rho}{\rho_P} - 1 \right) \cos \beta + (\psi - D(\beta, \mathcal{W})) \frac{\rho_P \sin \beta}{\rho} \right]. \quad (8)$$

Finally, let us define R as the set of all points in Ω_ℓ where $\dot{V} = 0$.

Next sections are dedicated to define the optimal control laws, v and ω , for any point on the motion plane, and to prove stability properties of the optimal feedback control scheme on the manifold M .

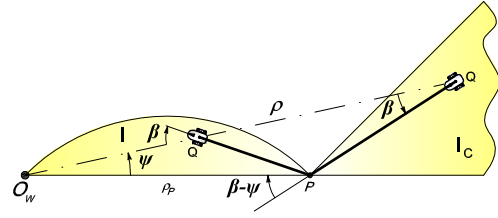


Fig. 4: Geometric construction to determine control law in Region I and I_c .

A. Control Laws

The key idea behind the control laws defined in this section, is to establish geometrical conditions that have to be respected to keep the vehicle aligned with optimal path in each point Q on the motion plane. As a consequence, with the proposed control laws the vehicle is able to perform the optimal path between the current robot position to the desired one, even if non-persistent drift occur in the command execution.

Although the optimal synthesis is completely defined in terms of only the state variables ρ and ψ , control laws are defined in terms of ρ , ψ and β , where $\beta \in \mathcal{W} = [-\phi, \phi]$. We will use superscript \mathcal{W} to make this explicit, (e.g., $I^{\mathcal{W}}$ corresponds to robot configuration $\eta = (\rho, \psi, \beta)$ such that point (ρ, ψ) belongs to Region I and angle $\beta \in \mathcal{W}$). Moreover, as control laws defined in next sections depend on geometrical properties of the optimal synthesis, they are not valid for values of $\beta \notin \mathcal{W}$ and, hence, it could not guarantee stability outside \mathcal{W} . For this reason, for η such that $\beta \notin \mathcal{W}$ and, hence $D(\beta, \mathcal{W}) \neq 0$, we consider the following control laws:

$$u(\eta) = \begin{cases} v = 0, \\ \omega = -K_\omega D(\beta, \mathcal{W}) \end{cases} \quad (9)$$

where K_ω is a positive control gain.

Finally, due to the symmetry of the optimal synthesis, we consider Q in the upper half plane (see figure 2), taking into account that a similar procedure can be followed to design control laws in each corresponding symmetric region.

1) *Control Law for Configuration $\eta \in I^{\mathcal{W}} \cup I_c^{\mathcal{W}}$* : for these robot configurations (see Table I), the optimal path to P is a straight line. From proposition 1, as for any point $Q \in I$ ($Q \in I_c$), point $P \in C_Q$ ($P \in \Gamma_Q$), vehicle follows optimal path if it is anytime aligned with segment \overline{QP} . Hence, based on figure 4, and by using the sine rule, we obtain the following alignment condition

$$F_{I^{\mathcal{W}} \cup I_c^{\mathcal{W}}}(\eta) = \frac{\rho}{\rho_P} \sin \beta - \sin(\beta - \psi) = 0 \quad (10)$$

Notice that, (10) depends on ratio $\frac{\rho}{\rho_P}$. As a consequence, it is also valid for state variables whose values are scaled by a common factor.

Based on (10) we are now able to define control law $u(\eta)$:

$$\omega = K_\omega \left(\frac{\rho}{\rho_P} \sin \beta - \sin(\beta - \psi) \right), \begin{cases} v = 0, & \text{if } F_{I^{\mathcal{W}} \cup I_c^{\mathcal{W}}}(\eta) \neq 0, \\ v = \bar{v}, & \text{if } F_{I^{\mathcal{W}} \cup I_c^{\mathcal{W}}}(\eta) = 0, \end{cases} \quad (11)$$

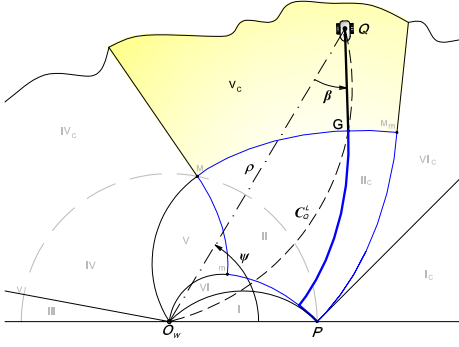


Fig. 5: Geometric construction to determine control law in Region V_c .

where K_ω is a positive control gain for points $Q \in I^{\mathcal{W}}$ and negative for points $Q \in I_c^{\mathcal{W}}$. In other words, the vehicle rotates on the spot until alignment condition $F_{I^{\mathcal{W}} \cup I_c^{\mathcal{W}}}(\eta) = 0$, and then follows straight line path toward P .

Remark 2: Notice that, when $F_{I^{\mathcal{W}} \cup I_c^{\mathcal{W}}}(\eta) = 0$ we still compute ω in order to correct the orientation error due to noise or drift, as usual happens in reality. This also happens for the following control laws.

2) *Control Law for Configuration $\eta \in VI_c^{\mathcal{W}}$:* for these robot configurations, the optimal path to P is of type $S^+T_p^{L+}$ (see Table I). For any $Q \in VI_c$, based on proposition 1, robot must move straight toward G , intersection between C_Q^L and spiral T_P^L (see figure 6), that is, recalling that $Q = (\rho, \psi)$, a solution of

$$F_{VI_c^{\mathcal{W}}}(\eta) = \frac{\rho \sin \beta}{\rho_P \sin \phi} + e^{(\psi - \beta - \phi)t} = 0, \quad (12)$$

in terms of β , where $t = 1/\tan \phi$. Based on (12) we are now able to define the control algorithm for points Q belonging to Region VI:

$$\omega = K_\omega \left(\frac{\rho \sin \beta}{\rho_P \sin \phi} + e^{(\psi - \beta - \phi)t} \right), \begin{cases} v = 0, & \text{if } F_{VI_c^{\mathcal{W}}}(\eta) \neq 0, \\ v = \bar{v}, & \text{if } F_{VI_c^{\mathcal{W}}}(\eta) = 0, \end{cases}$$

with $K_\omega > 0$.

3) *Control Law for Configuration $\eta \in V_c^{\mathcal{W}}$:* if robot position is in regions V_c (see figure 2), with $\beta \in \mathcal{W}$, for these robot configurations, the shortest path to P is of type $S^+T^{L+} * T_p^{R-}$ (see Table I). From points $Q \in V_c$, for proposition 1, vehicle must move toward the intersection point between spiral T_M^R and C_Q^L (see figure 5), that is a solution of

$$F_{V_c^{\mathcal{W}}}(\eta) = \frac{\rho \sin \beta}{\rho_P \sin \phi} + e^{(\psi_M - \psi + \beta + \phi)t} = 0, \quad (13)$$

in terms of β , where $\psi_M = -4 \tan \phi \ln \sin \phi$ and $t = 1/\tan \phi$. Notice that, (13) is valid for state variables whose values are scaled by a common factor. Based on (13) we are now able to define the control algorithm for points Q belonging to Region V_c :

$$\omega = K_\omega \left(\frac{\rho \sin \beta}{\rho_P \sin \phi} + e^{(\psi_M - \psi + \beta + \phi)t} \right), \begin{cases} v = 0, & \text{if } F_{V_c^{\mathcal{W}}}(\eta) \neq 0, \\ v = \bar{v}, & \text{if } F_{V_c^{\mathcal{W}}}(\eta) = 0, \end{cases}$$

where $K_\omega > 0$.

4) *Control Law for Configuration $\eta \in IV^{\mathcal{W}} \cup IV_c^{\mathcal{W}}$:* from these robot configurations, the optimal path to P is of type $S^+T^{L+} * T^{R-}S^-$ (see Table I). Based on proposition 1, from these points, vehicle has to be aligned with segment QG , where G is the intersection point between C_Q^L and C_M^R (see figure 6). In other words, given a point Q in Region $IV \cup IV_c$, alignment condition can be obtained as solution of

$$F_{IV^{\mathcal{W}} \cup IV_c^{\mathcal{W}}}(\eta) = \sin(2\phi + \psi_M + \beta - \psi) + \frac{\rho}{\rho_P} \sin \beta = 0, \quad (14)$$

in terms of β , where $\psi_M = -4 \tan \phi \ln \sin \phi$. Notice that, (14) is valid for state variables whose values are scaled by a common factor. Based on (14) we are now able to define the control laws:

$$\omega = K_\omega \left(\sin(2\phi + \psi_M + \beta - \psi) + \frac{\rho}{\rho_P} \sin \beta \right), \begin{cases} v = 0, & \text{if } F_{IV^{\mathcal{W}} \cup IV_c^{\mathcal{W}}}(\eta) \neq 0, \\ v = \bar{v}, & \text{if } F_{IV^{\mathcal{W}} \cup IV_c^{\mathcal{W}}}(\eta) = 0, \end{cases}$$

where $K_\omega > 0$.

5) *Control Law for Configuration $\eta \in II_c^{\mathcal{W}} \cup II^{\mathcal{W}} \cup II_c^{\mathcal{W}} \cup V^{\mathcal{W}}$:* from these robot configurations, the robot must move along a T_Q^{L+} spiral arc. The vehicle is aligned with a left logarithmic spiral if angle β is equal to spiral's characteristic angle, i.e., $\beta = \phi$. Hence, the control laws for such points are

$$\omega = -K_\omega(\beta + \phi) + \frac{\sin \beta}{\rho} v, \begin{cases} v = 0, & \text{if } \beta + \phi \neq 0, \\ v = \bar{v}, & \text{if } \beta + \phi = 0, \end{cases}$$

where $K_\omega > 0$. Unfortunately, for geometrical properties of the logarithmic spirals, it is not possible to move along spirals with a feedback control computed on state variables known up to a common scale factor (notice that this occurs also for a circumference). Hence, a further knowledge about feature position is necessary to perform this path, for example height of the feature that is kept in sight during motion.

6) *Control Law for Configuration $\eta \in II^{\mathcal{W}} \cup VI^{\mathcal{W}}$:* if robot configuration η is such that point $Q = (\rho, \psi)$ belongs to regions $II^{\mathcal{W}} \cup VI^{\mathcal{W}}$, with $\beta \in \mathcal{W}$, from these robot configurations, the robot must move along a T_Q^{R-} spiral arc. The vehicle is aligned with a right logarithmic spiral if angle β is equal to spiral's characteristic angle, i.e., $\beta = -\phi$. Hence, the control laws for such points are

$$\omega = -K_\omega(\beta - \phi) + \frac{\sin \beta}{\rho} v, \begin{cases} v = 0, & \text{if } \beta - \phi \neq 0, \\ v = \bar{v}, & \text{if } \beta - \phi = 0, \end{cases}$$

where $K_\omega > 0$.

7) *Control Law for Configuration $\eta \in III^{\mathcal{W}} \cup III_c^{\mathcal{W}}$:* if robot configuration η is such that point $Q = (\rho, \psi)$ belongs to regions $III^{\mathcal{W}} \cup III_c^{\mathcal{W}}$, with $\beta \in \mathcal{W}$, in this particular case, the robot must move toward feature position O_W . The vehicle is aligned with the straight line from Q to O_W if $\beta = 0$; hence, control laws are

$$\omega = K_\omega \beta, \begin{cases} v = 0, & \text{if } \beta \neq 0, \\ v = \bar{v}, & \text{if } \beta = 0, \end{cases}$$

where $K_\omega > 0$. Notice that, v defined in (8), has a singularity in O_W . Indeed, in O_W variables β and ψ are not defined and $\rho = 0$. In this case is however still possible to define control laws that brings the robot in region VI (or I) without

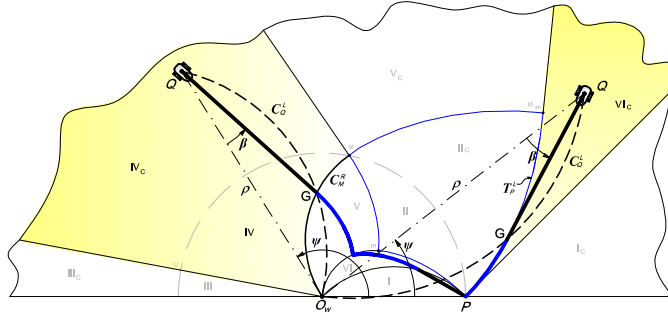


Fig. 6: Geometric construction to determine control law in Region $IV \cup IV_c$ and Region VI_c .

following the optimal path in order to avoid the crossing of O_W .

IV. STABILITY ANALYSIS

In this section, the stability of the control scheme previously presented is analyzed by means of a generalization of the LaSalle's invariance principle for discontinuous righthand systems [16], showing that manifold $M = \{\eta \in \mathbb{R}^3 | \rho = \rho_P, \psi = 0, \beta \in \mathcal{W}\}$ is asymptotically stable for any initial configuration of the robot on the motion plane.

The objective here is to prove that the largest invariant set in $R = \{\eta \in \mathbb{R}^3 | \dot{V}(\eta) = 0\}$ in Ω_ℓ is the manifold M . Next section are dedicated to characterized set R for each region and then determine the largest invariant set in Ω_ℓ . For the sake of clarity, for each region we consider only points in Ω_ℓ omitting this intersection in the following notation.

For points Q such that $\beta \notin \mathcal{W}$, i.e. $D(\beta, \mathcal{W}) \neq 0$, $\dot{V}(\eta) = -K_\omega D^2(\beta, \mathcal{W})$, that is negative semidefinite. Set of points Q such that $\dot{V}(\eta) = 0$ is given by $R_{\beta \notin \mathcal{W}} = \{D(\beta, \mathcal{W}) = 0, \forall \rho, \forall \psi\}$, i.e., set of points whose stability will now be analyzed.

For all points Q such that $\beta \in \mathcal{W}$, (7) becomes

$$\dot{V}(\eta) = \frac{1}{\rho_P} \left[- \left(\frac{\rho}{\rho_P} - 1 \right) \cos \beta + \psi \frac{\rho_P \sin \beta}{\rho} \right] v, \quad (15)$$

that depends only on input control v . Notice that, since $D(\beta, \mathcal{W}) = 0$, the control input v is the same for all the regions of the optimal synthesis and

$$\dot{V}(\eta) = -\frac{K_V}{\rho_P} \left[- \left(\frac{\rho}{\rho_P} - 1 \right) \cos \beta + \psi \frac{\rho_P \sin \beta}{\rho} \right]^2. \quad (16)$$

The set of points Q with $\beta \in \mathcal{W}$ and such that $\dot{V}(\eta) = 0$ is $R_{\beta \in \mathcal{W}} = M \cup \{\psi = 0, \beta = \pi/2, \forall \rho\} \cup \{\beta = \arctan \left(\left(\frac{\rho}{\rho_P} - 1 \right) \frac{\rho}{\rho_P \psi} \right), \forall \psi, \forall \rho\}$.

The objective now is to characterize the largest invariant set contained in $R_{\beta \in \mathcal{W}}$.

Proposition 2: The largest invariance set contained in $R = R_{\beta \notin \mathcal{W}} \cup R_{\beta \in \mathcal{W}}$ is $M = \{\eta \in \mathbb{R}^3 | \rho = \rho_P, \psi = 0, \beta \in \mathcal{W}\}$.

Proof: Previous results for point Q such that $\beta \in \mathcal{W}$ prove that starting from $R_{\beta \notin \mathcal{W}}$, the system evolves in $R_{\beta \in \mathcal{W}}$. Hence, $R_{\beta \notin \mathcal{W}}$ does not contain invariant sets.

For any Q such that $\beta = \arctan \left(\left(\frac{\rho}{\rho_P} - 1 \right) \frac{\rho}{\rho_P \psi} \right)$, we have $\dot{V}(\eta) = 0$ and hence $v = 0$. As a consequence, from the

kinematic model, $\dot{\rho} = \dot{\psi} = 0$ and hence β should be constant. From the control laws defined previously, this happens only if β is such that the robot is aligned with the optimal path associated to the region it belongs to. It can be directly verified that such values of β do not verify alignment conditions reported above. Hence, the considered subset of R does not contain invariant sets.

Set $R_1 = \{\psi = 0, \beta = \pi/2, \forall \rho\}$ is a subset of $I^{\mathcal{W}} \cup I_c^{\mathcal{W}}$. Hence, for any Q in R_1 , (10) becomes $F_{I^{\mathcal{W}} \cup I_c^{\mathcal{W}}} = \frac{\rho}{\rho_P} - 1$. If $\rho \neq \rho_P$ the control laws are $v = 0$ and $\omega \neq 0$. Hence, $\dot{\beta} \neq 0$ and R_1 does not contain invariant sets.

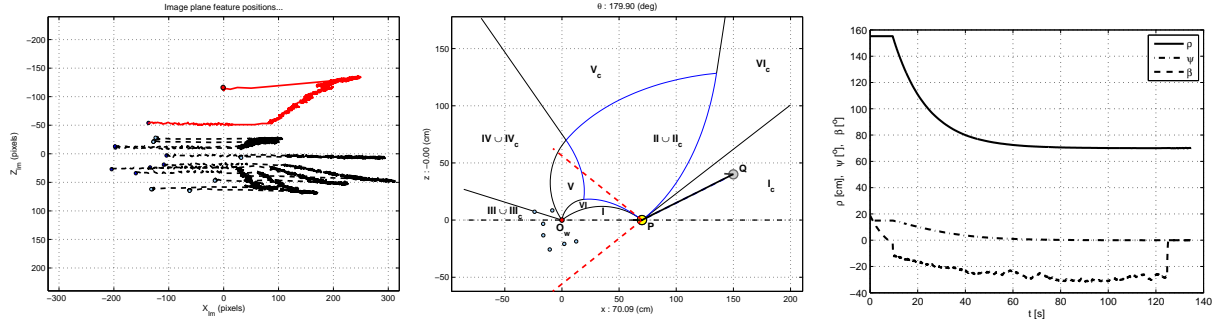
If $Q \in R_1$ and $\rho_Q = \rho_P$ we have that Q is a particular point of M . Finally, notice that $M \subset I^{\mathcal{W}}$, and for any $Q \in M$ $F_{I^{\mathcal{W}} \cup I_c^{\mathcal{W}}} = 0$. From control laws 11 we have $v = \omega = 0$ hence M is an invariant set. ■

As the control laws are derived from the optimal synthesis which is discontinuous, then also the closed-loop system is discontinuous. Nevertheless, existence and uniqueness of solutions are guaranteed by Filippov existence theorem (see [11]) and the control laws choice in previous section. By using a generalization of LaSalle's invariance principle for discontinuous righthand systems [16] and proposition 2, M is stable for the optimal feedback control laws previously defined.

V. SIMULATION RESULTS

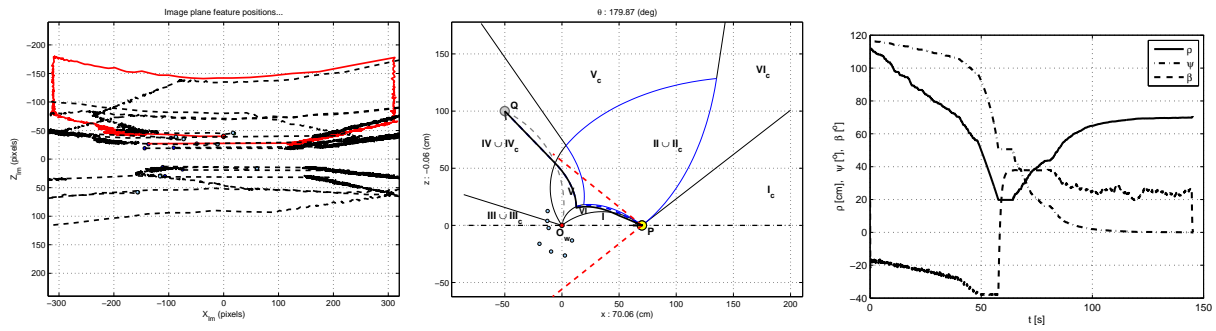
In this section, simulated results are presented showing the effectiveness of control laws proposed in this paper.

A virtual framework is used where random 3-D points representing features of a virtual scene are generated. The 3-D points of the scene are projected in the image plane of a virtual camera whose size is 640×480 pixels. Moreover, the image frames are captured with 10 frames/second. The characteristic angle of the symmetric planar cone is $\delta = 2\phi = 37.76^\circ$. The control laws proposed in this paper are designed to keep only one landmark in view. Nevertheless, before moving toward desired position P along the optimal path, vehicle needs to localize itself by the estimate of ψ and ratio ρ/ρ_P by using feature measurements on the image plane. In order to do this at least three features in view are needed. For this reason, we will generate several virtual points in the scene to guarantee this requirement anytime during all maneuvers that robot performs along the shortest path. Once the vehicle is localized, the associated controller is selected



(a) On the left: features trajectories on the image plane (solid line for O_w , dashed line for others). On the right: robot trajectory on the motion plane from $Q \in I^{\mathcal{W}}$ (solid line for real trajectory, dashed line for the ideal one). (b) Evolution of state variables ρ , ψ and β .

Fig. 7: Optimal path from points Q in Region I (S^+) ($Q = [155.24, 15^\circ, 12.6^\circ]^T$ and $P = [70, 0^\circ, 0^\circ]^T$).



(a) On the left: features trajectories on the image plane (solid line for O_w , dashed line for others). On the right: robot trajectory on the motion plane from $Q \in IV^{\mathcal{W}} \cup IV_c^{\mathcal{W}}$ (solid line for real trajectory, dashed line for the ideal one). (b) Evolution of state variables ρ , ψ and β .

Fig. 8: Optimal path from points Q in Region $IV \cup IV_c$ ($S^+T^{-}L^+ * T^{-}R^{-}S^-$) ($Q = [111.8, 116.5^\circ, 0^\circ]^T$ and $P = [70, 0^\circ, 0^\circ]^T$).

and performed. Control laws for configurations η in Regions $I^{\mathcal{W}}$, $I_c^{\mathcal{W}}$, $VI_c^{\mathcal{W}}$, $V_c^{\mathcal{W}}$, $IV^{\mathcal{W}} \cup IV_c^{\mathcal{W}}$ and $III^{\mathcal{W}} \cup III_c^{\mathcal{W}}$ are defined in terms of β and ratio ρ/ρ_P which can be determined by using directly image coordinates of only one feature and ψ which can be determine as in [6] by using at least three image feature coordinates. On the other hand, for control laws in Regions $II^{\mathcal{W}}$, $II_c^{\mathcal{W}}$, $II^{\mathcal{W}}$, $II_c^{\mathcal{W}}$ and $VI^{\mathcal{W}}$, input ω is defined in terms of the absolute value of ρ which can be obtained by using directly image coordinates of only one feature but assuming, as in this paper, that the height of the feature is known. For this reason, the visual servoing approach proposed here can be classified as a combination of Image-Based and Position-Based approach depending on which Region robot is in.

Simulations reported here concern the optimal feedback control laws from points Q in Region I_c (see figure 7) and Region $IV \cup IV_c$ (see figure 8). Figures show also feature trajectories on image plane (see [14] for correspondences between image trajectories and extremal arc followed by the vehicle). Notice that, when the vehicle performs a logarithmic spiral the reference feature in O_w should move along the left or the right border of the image plane. From a practical point of view, a small deviation in the wrong direction causes the robot to lost the feature. For this reason, we assume

that during spiral motions the feature in O_w moves along a line parallel to the left or the right border, at a distance of 10 pixels (e.g., figure 8).

Simulations are performed adding Gaussian image noise to the points with a standard deviation of $\sigma = 0.3$ pixels. Moreover, as typically done in simulations, in order to avoid a jerky behavior of the real robot (e.g., in our case the linear velocity assumes a non-zero value only if the robot is perfectly aligned with the optimal vector field) we implement a dead zone around the switching condition in which the linear velocity is non zero. In addition, in order to keep the vehicle aligned to the path the linear velocity may need to be reduced with respect to the angular velocity. In this case the linear velocity can be changed, through K_v , without affecting the optimality of the trajectory that is minimized in terms of length and not in terms of time.

As previously said, for self-localization at least two features in addition to the reference one in O_w must be kept in view along shortest path from any Q to P . These features can be chosen arbitrarily at any moment and they need to be tracked during the servoing task. In other words, if a feature is lost it is sufficient to chose another feature in view in order to have a correct robot localization.

Finally, when robot reaches desired position P , the control

law $u(\eta) = [0, K_\omega \beta]$ is performed in order to align the vehicle with the desired orientation.

VI. CONCLUSION AND FUTURE WORKS

A nonlinear optimal feedback control capable of maintaining the vehicle aligned with shortest path from any initial robot position to the desired one has been proposed. Moreover, a proof of stability has been given and realistic simulations, assuming feature noise and loss of features, have been reported, proving the effectiveness of our technique. However, experiments on a real nonholonomic robot platform must be done to prove the effectiveness of the proposed control laws in realistic conditions and is left to future works. In this paper, the problem of keeping in sight, during motion, at least one feature has been taken into account. On the other hand, in order to obtain the current robot position, at least three features are needed. As a consequence, a generalization of the optimal synthesis used in this paper to define the shortest paths to a goal keeping in sight at least three features. Such extension to the proposed approach is still an open problem. Furthermore, only horizontal FOV limits have been taken into account; a further generalization will be to consider also vertical FOV limits which prevent the vehicle to reach points in a neighborhood of landmarks.

REFERENCES

- [1] F. Chaumette and S. Hutchinson, "Visual servo control, Part I: Basic approaches," *IEEE Robotics and Automation Magazine*, vol. 13, no. 4, pp. 82–90, December 2006.
- [2] —, "Visual servo control, Part II: Advanced approaches," *IEEE Robotics and Automation Magazine*, vol. 14, no. 1, pp. 109–118, March 2007.
- [3] A. C. Sanderson and L. E. Weiss, "Image-based visual servo control using relational graph error signals," in *Proc. IEEE Int. Conf. on Robotics and Automation*, 1980, pp. 1074–1077.
- [4] G. L. Mariottini, G. Oriolo, and D. Prattichizzo, "Image-based visual servoing for nonholonomic mobile robots using epipolar geometry," *Robotics, IEEE Transactions on*, vol. 23, no. 1, pp. 87–100, feb 2007.
- [5] G. López-Nicolás, C. Sagüés, J. Guerrero, D. Kragic, and P. Jensfelt, "Switching visual control based on epipoles for mobile robots," *Robotics and Autonomous Systems*, vol. 56, no. 7, pp. 592–603, 2008.
- [6] X. Zhang, Y. Fang, and X. Liu, "Visual servoing of nonholonomic mobile robots based on a new motion estimation technique," in *Decision and Control, 2009 held jointly with the 2009 28th Chinese Control Conference. CDC/CCC 2009. Proceedings of the 48th IEEE Conference on*, dec 2009, pp. 8428–8433.
- [7] P. Murrieri, D. Fontanelli, and A. Bicchi, "A hybrid-control approach to the parking problem of a wheeled vehicle using limited view-angle visual feedback," *Int. Jour. of Robotics Research*, vol. 23, no. 4–5, pp. 437–448, April–May 2004.
- [8] N. Gans and S. Hutchinson, "Stable visual servoing through hybrid switched system control," *IEEE Transactions on Robotics*, vol. 23, no. 3, pp. 530–540, June 2007.
- [9] —, "A stable vision-based control scheme for nonholonomic vehicles to keep a landmark in the field of view," in *Proc. IEEE Int. Conf. on Robotics and Automation*, apr. 2007, pp. 2196–2201.
- [10] S. Bhattacharya, R. Murrieta-Cid, and S. Hutchinson, "Optimal paths for landmark-based navigation by differential-drive vehicles with field-of-view constraints," *IEEE Transactions on Robotics*, vol. 23, no. 1, pp. 47–59, February 2007.
- [11] P. Salaris, D. Fontanelli, L. Pallottino, and A. Bicchi, "Shortest paths for a robot with nonholonomic and field-of-view constraints," *IEEE Transactions on Robotics*, vol. 26, no. 2, pp. 269–281, April 2010.
- [12] G. Lopez-Nicolas, N. Gans, S. Bhattacharya, C. Sague, J. Guerrero, and S. Hutchinson, "Homography-based control scheme for mobile robots with nonholonomic and field-of-view constraints," *Systems, Man, and Cybernetics, Part B: Cybernetics, IEEE Transactions on*, vol. 40, no. 4, pp. 1115–1127, Aug 2010.
- [13] P. Lucibello and G. Oriolo, "Stabilization via iterative state steering with application to chained-form systems," in *Decision and Control, 1996., Proceedings of the 35th IEEE*, vol. 3, dec 1996, pp. 2614–2619.
- [14] P. Salaris, F. A. W. Belo, D. Fontanelli, L. Greco, and A. Bicchi, "Optimal paths in a constrained image plane for purely image-based parking," *IROS*, pp. 1673–1680, 2008.
- [15] S. Arimoto, J.-H. Bae, and K. Tahara, "Stability on a manifold: simultaneous realization of grasp and orientation control of an object by a pair of robot fingers," in *Robotics and Automation, 2003. Proceedings. ICRA '03. IEEE International Conference on*, vol. 2, sept 2003, pp. 2336–2343.
- [16] A. Bacciotti and F. Ceragioli, "Stability and stabilization of discontinuous systems and nonsmooth Lyapunov functions," *ESAIM: Control, Optimisation and Calculus of Variations*, vol. 4, pp. 361–376, 1999.
- [17] P. Salaris, D. Fontanelli, L. Pallottino, and A. Bicchi, "Optimal paths for mobile robots with limited field of view camera," in *48th IEEE Conference on Decision and Control*, Dec 2009, pp. 8434–8439.
- [18] A. Bryson and Y. Ho, *Applied optimal control*. Wiley New York, 1975.
- [19] X. Zhang, Y. Fang, and X. Liu, "Visual servoing of nonholonomic mobile robots based on a new motion estimation technique," in *Decision and Control, 2009 held jointly with the 2009 28th Chinese Control Conference. CDC/CCC 2009. Proceedings of the 48th IEEE Conference on*, dec 2009, pp. 8428–8433.